Electronic Supplementary Material (ESI) for Materials Chemistry Frontiers.

Mechanism of Ligand-Induced Chiral Transmission Through a Top-Down Selective Domain Etching

Junjie Hao,[1,2#] Junzi Li,[3#] Meijuan Chen,[2,4] Xijian Duan,[2,5,6] Bing Xu,[6] Yiwen Li,[4] Tingchao He,[3*] Xiao Wei Sun,[2,5,6*] Marie-Hélène Delville,[1*] Jiaji Cheng[4*]

[1] CNRS, Univ. Bordeaux, Bordeaux INP, ICMCB, UMR 5026, Pessac, F-33608, France;
[2] Key Laboratory of Energy Conversion and Storage Technologies (Southern University of Science and Technology), Ministry of Education, Shenzhen 518055, China;
[3] College of Physics and Optoelectronic Engineering, Shenzhen University, Shenzhen, Guangdong 518060, China;
[4] School of Materials Science and Engineering, Hubei University, Wuhan, Hubei 430062, China;
[5] Guangdong University Key Laboratory for Advanced Quantum Dot Displays and Lighting, Guangdong-Hong Kong-Macao Joint Laboratory for Photonic-Thermal-Electrical Energy Materials and Devices, Shenzhen Key Laboratory for Advanced Quantum Dot Displays and Lighting, SUSTech-HUAWEI Joint Lab for Photonics Industry, and Department of Electrical and Electronic Engineering, Southern University of Science and Technology, Shenzhen 518055, China;
[6] Shenzhen Planck Innovation Technologies Co. Ltd., Shenzhen 518055, China.
 # These authors contributed equally to this work.
Email: jiajicheng@hubu.edu.cn; marie-helene.delville@icmcb.cnrs.fr; sunxw@sustech.edu.cn; tche@szu.edu.cn

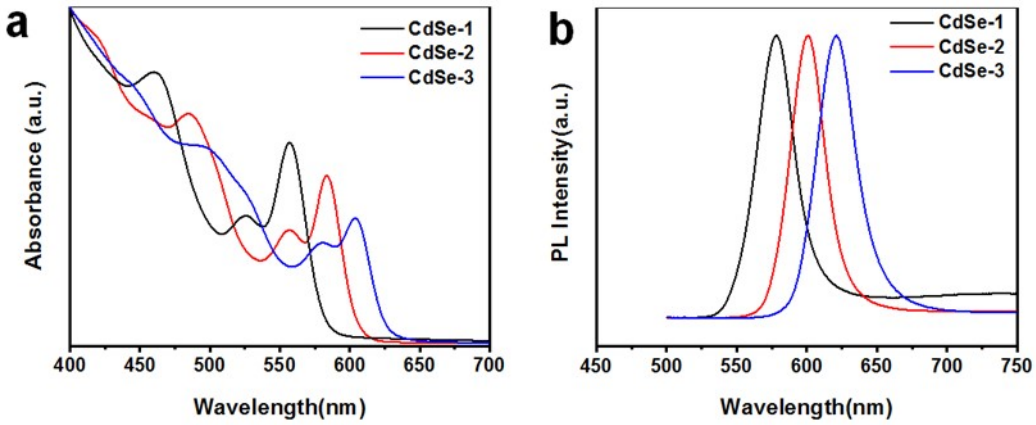

Figure S1. UV-vis. and PL of the different CdSe cores for the control synthesis of DRs.

Table S1. Physical properties of different CdSe cores.

Name	Abs (nm)	Diameter (nm)[a]	PL (nm)	FWHM (nm)
CdSe-1	557	3.2	578	33
CdSe-2	583	3.9	601	30
CdSe-3	603	4.7	619	32

[a] Diameter of the CdSe core is determined from the absorption spectrum by Peng's equation (nm).[1]

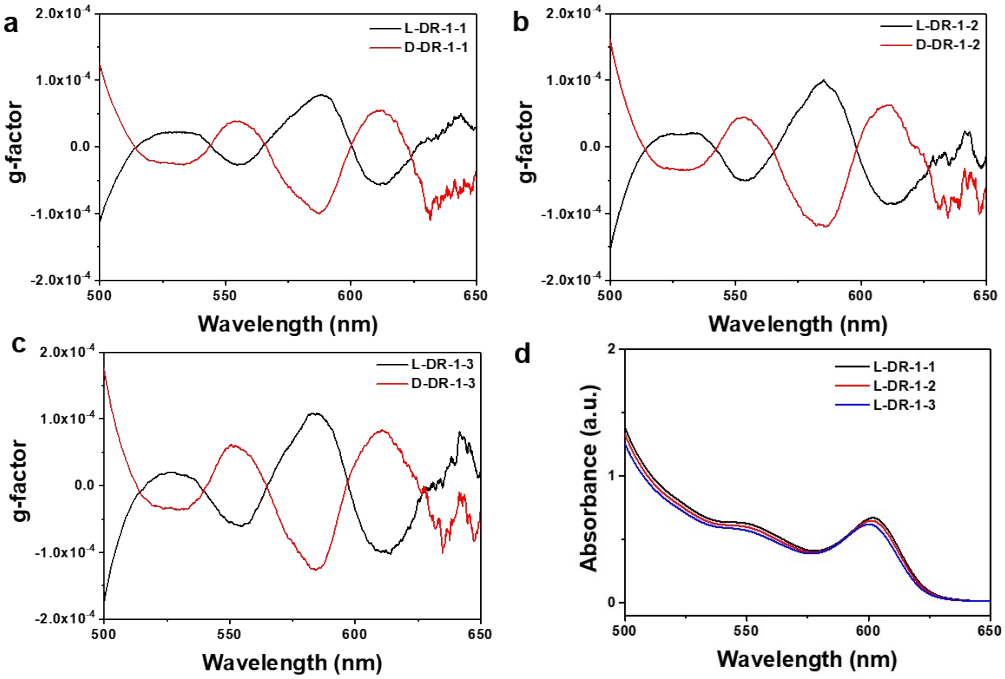

Figure S2. Corresponding g-factors variations and UV-vis. spectra of DR-1-n (n = 1-3) at the first exciton absorption peak as shown in Figure 4. a) CD spectrum of benzylamine modified DRs-1-1 after Cys exchange; b) CD spectrum of DRs-1-2 after one etching cycle and Cys exchange; c) CD spectrum of DRs-1-3 after two etching cycles and Cys exchange; d) Corresponding UV-vis. absorption spectra of the different etching processes.

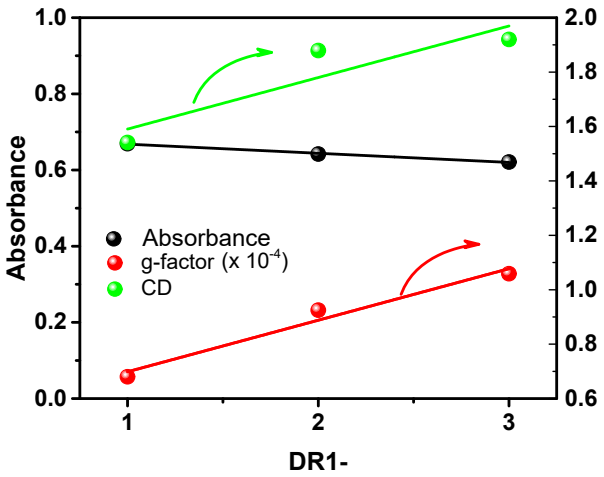

Figure S3. CD, UV-vis. and g-factor variations of L-Cys-DR-1-3 (n= 1-3) at the first exciton absorption peak during the etching process. The UV-vis. value was taken at the maximum at the first exciton absorption peak.

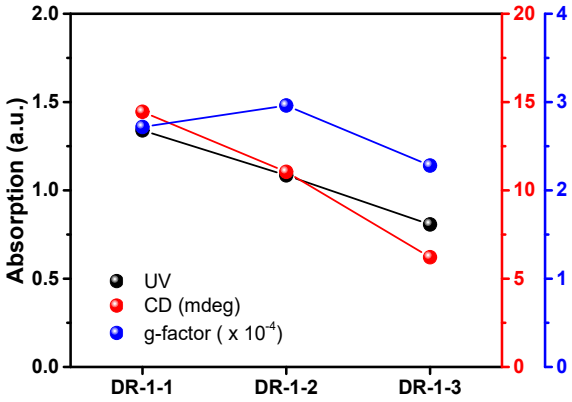

Figure S4. CD, UV-vis. and g-factor evolution of L-Cys-DR-1 (< 500 nm) during the etching process. The UV-vis. value is the wavelength of the maximum value of the CD signal.

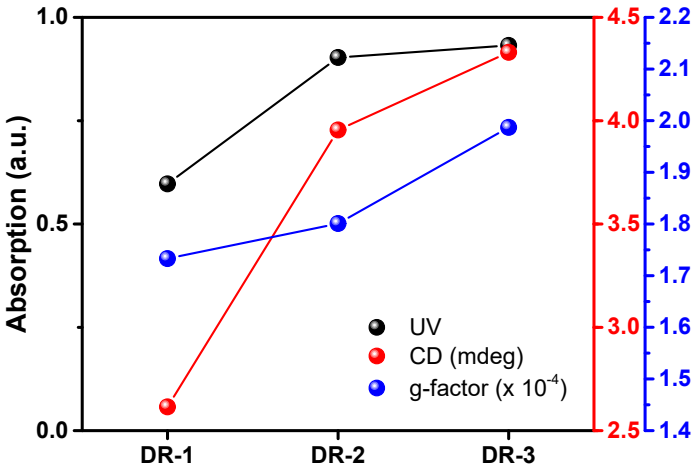

Figure S5. CD, UV-vis. and g-factor variations of L-Cys-DRs with different shell thicknesses at the first exciton absorption peak. The UV-vis. value is the maximum value at the first exciton absorption peak.

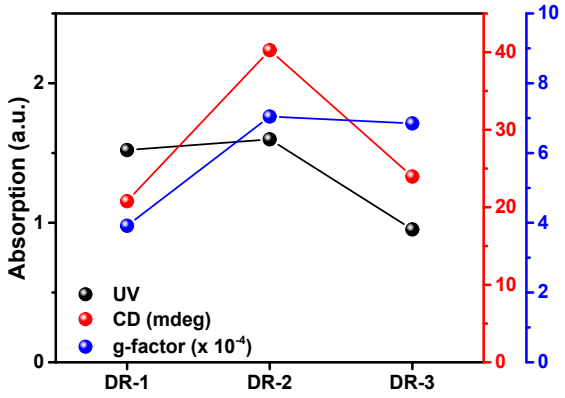

Figure S6. CD, UV-vis. and g-factor variations of L-Cys-DRs with different shell thicknesses (< 500 nm). The UV-vis. value is the wavelength of the maximum value of the CD signal.

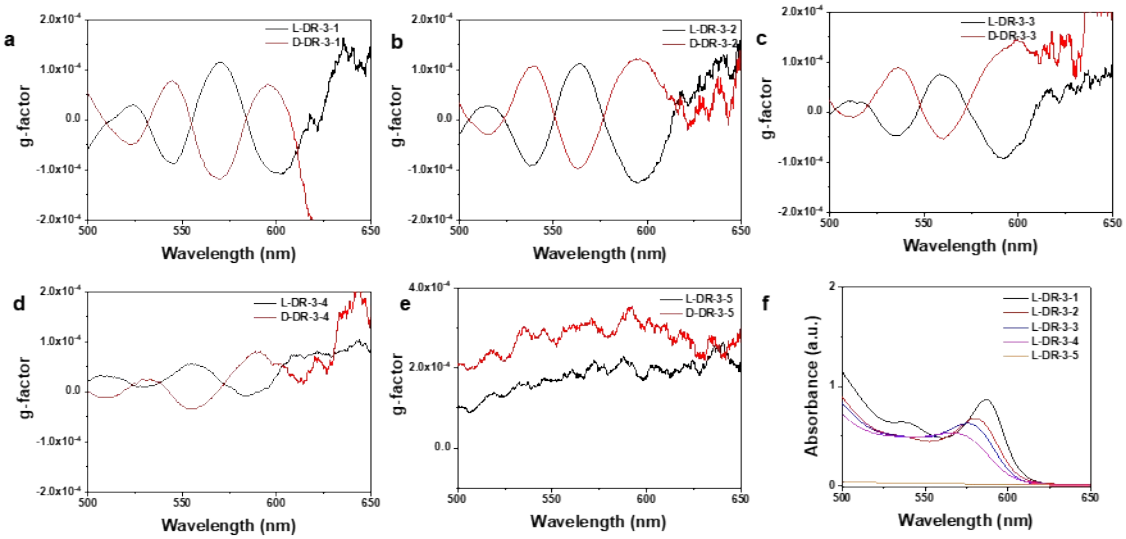

Figure S7. Corresponding UV-vis. and g-factor variations of DR-3 at the first exciton absorption peak as shown in Figure 8. (a) CD spectrum of benzyl amine-modified DRs after Cys exchange, (b)-(e) CD spectra of DRs with one cycle to four etching cycles after Cys exchange, (f) Corresponding UV-vis. absorptions of the different etching processes.

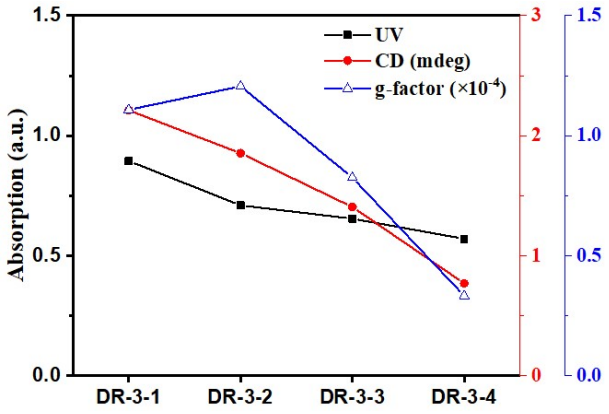

Figure S8. CD, UV-vis. and g-factor variations of L-Cys-DR-3-n (n = 1-4) at the first exciton absorption peak during the etching process. The UV-vis. value is the maximum value at the first exciton absorption peak.

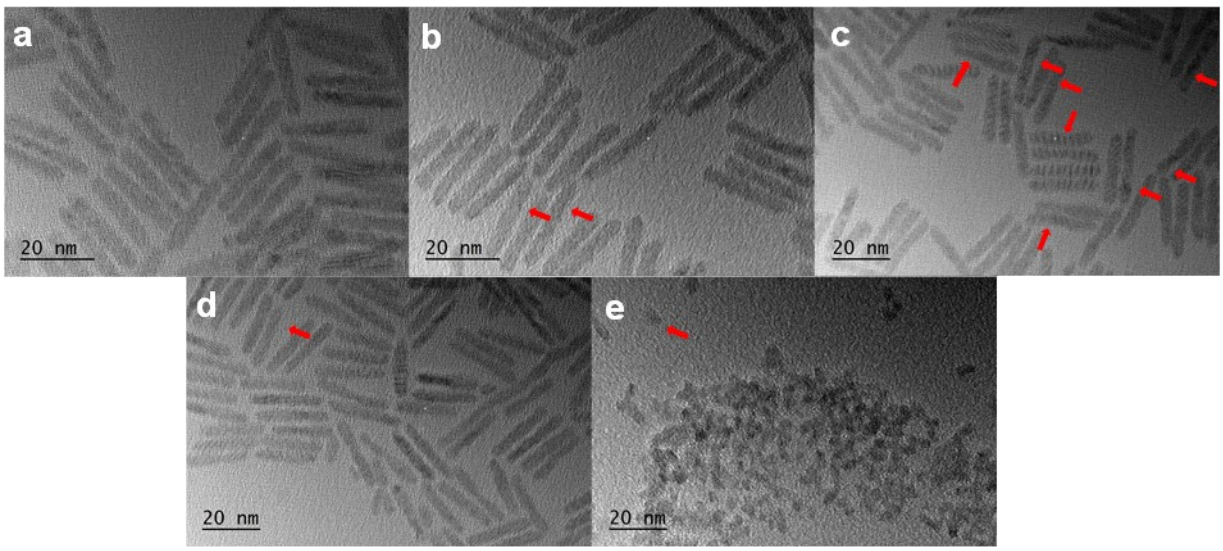

Figure S9. TEM images of DR-3 after the etching process. a) TEM of benzylamine modified DRs; b)-e) TEM of DRs after one cycle to four etching cycles.

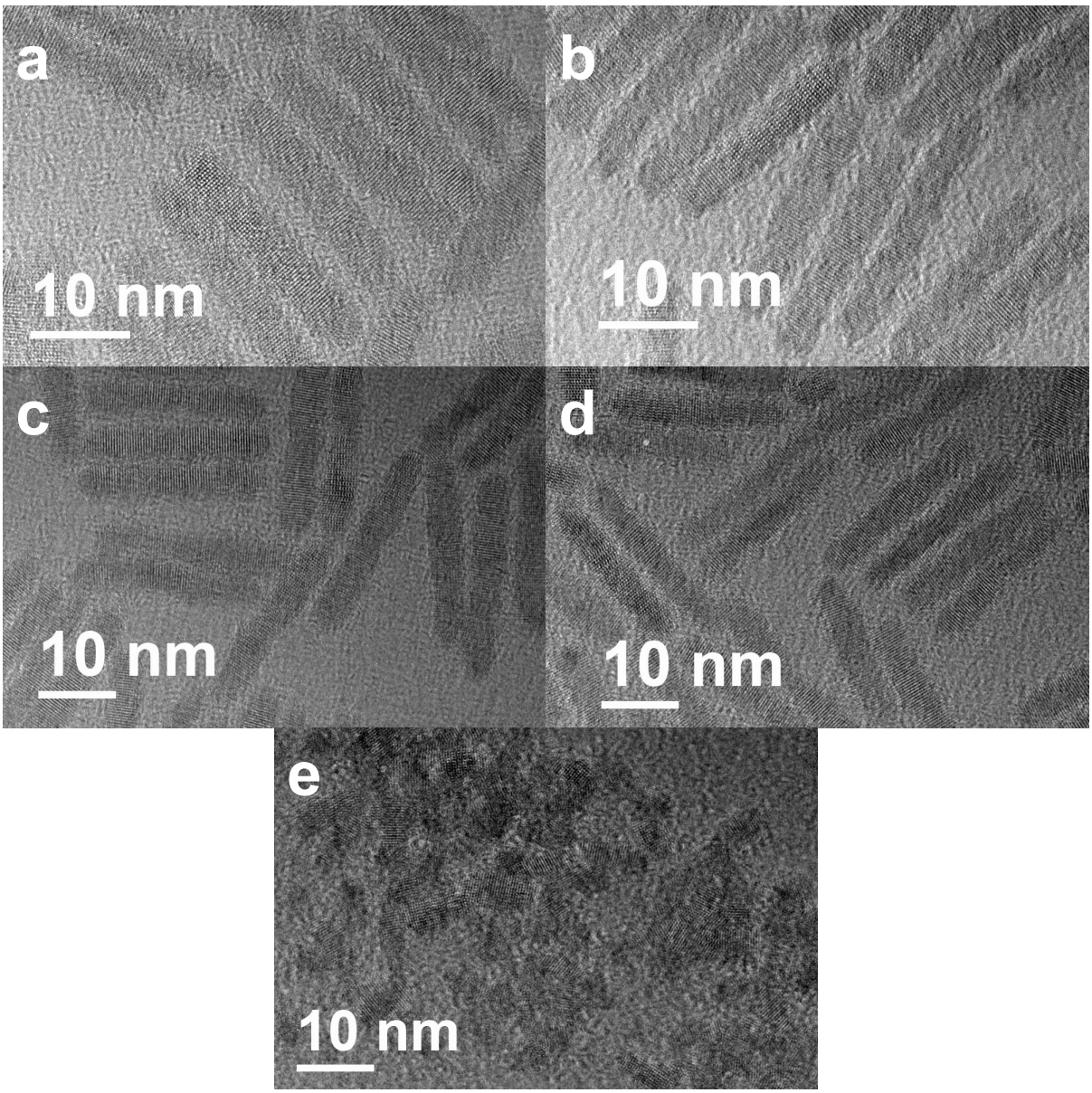

Figure S10. The HRTEM images corresponding to Figure 9. a) HRTEM of benzylamine modified DRs; b)-e) HRTEM of DRs after one cycle to four etching cycles.

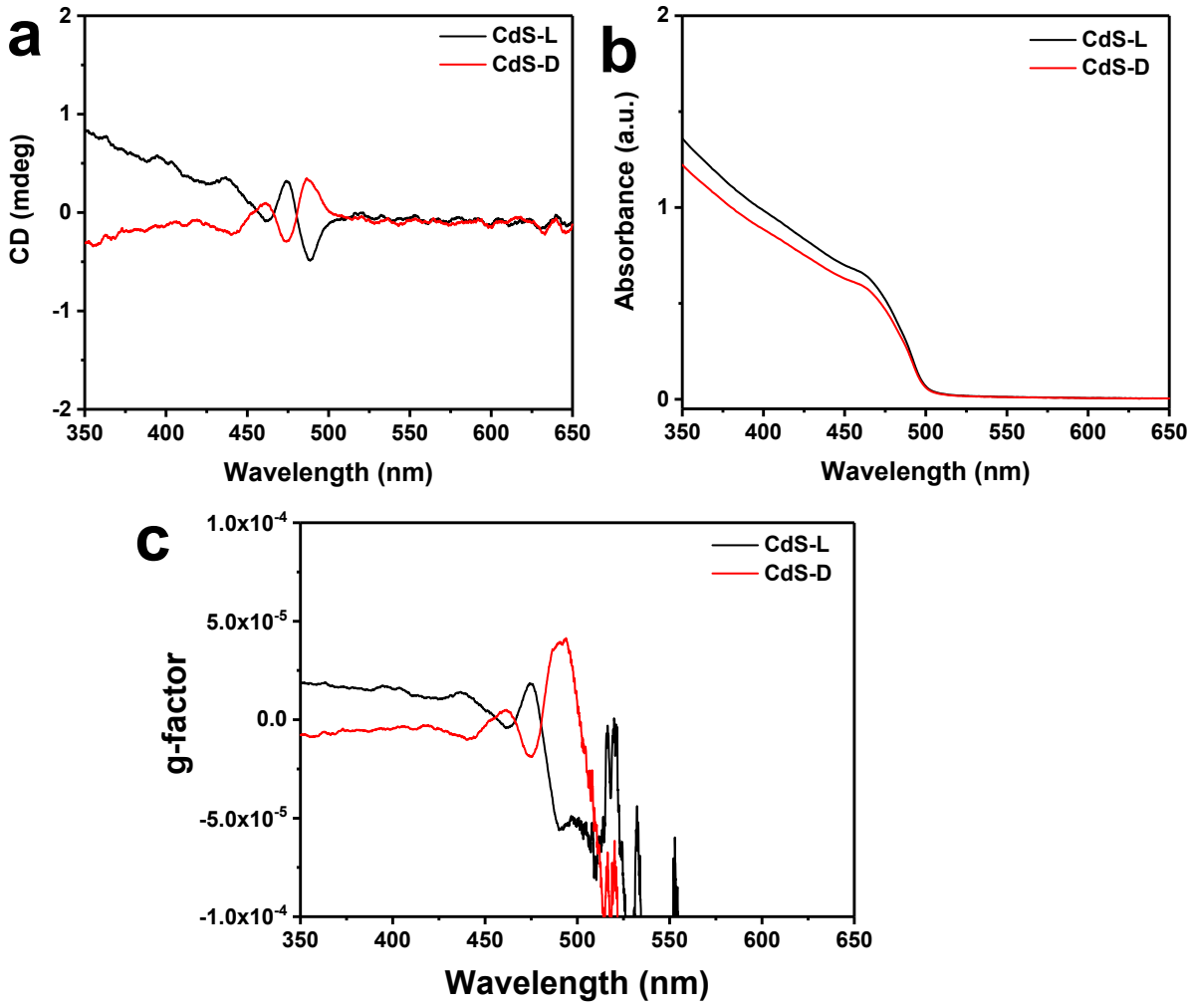

Figure S11. a) The CD spectrum of CdS-only nanorods after Cys exchange; b) the Corresponding UV-vis. absorptions of L-/D-CdS-only nanorods; c) the corresponding g-factor L-/D-CdS-only nanorods. The g_{CD} factor, defined as $|g_{CD+} - g_{CD-}|/2$, are 3.72×10^{-5} and 3.00×10^{-5} for L- and D-CdS-only nanorods, respectively.

Table S2. CD and g-factor of L-Cys-DR-3 at the first exciton absorption peak during the etching process.

Name	UV-vis (nm)	CD^+/λ_{CD}[a]	CD^-/λ_{CD}[b]	$\lvert CD^+ - CD^- \rvert/2$[c]	g_{CD+}/λ_{CD}[d]	g_{CD-}/λ_{CD}[e]	$\lvert g_{CD+} - g_{CD-} \rvert/2$[f]
DR-3-1	586.8	2.251/572.0	-2.170/593.6	2.211	1.161/569.2	-1.055/599.4	1.108
DR-3-2	580.2	1.991/565.0	-2.093/589.6	1.853	1.135/563.4	-1.276/595.0	1.206
DR-3-3	575.0	1.402/558.0	-1.412/586.6	1.407	0.735/559.4	-0.915/591.6	0.825
DR-3-4	568.8	1.354/555.0	-0.185/582.2	0.770	0.566/554.8	-0.099/583.0	0.333
DR-3-5	/	/	/	/	/	/	/

[a, b] CD anisotropy at the most intense positive and negative CD bands (mdeg/nm), [c] magnitude of the CD signal, defined as $|CD^+ - CD^-|/2$, [d, e] CD anisotropy g_{CD}-factors at the most intense positive and negative CD bands (10^{-4}/nm), [f] magnitude of the g_{CD} factor, defined as $|g_{CD+} - g_{CD-}|/2$.

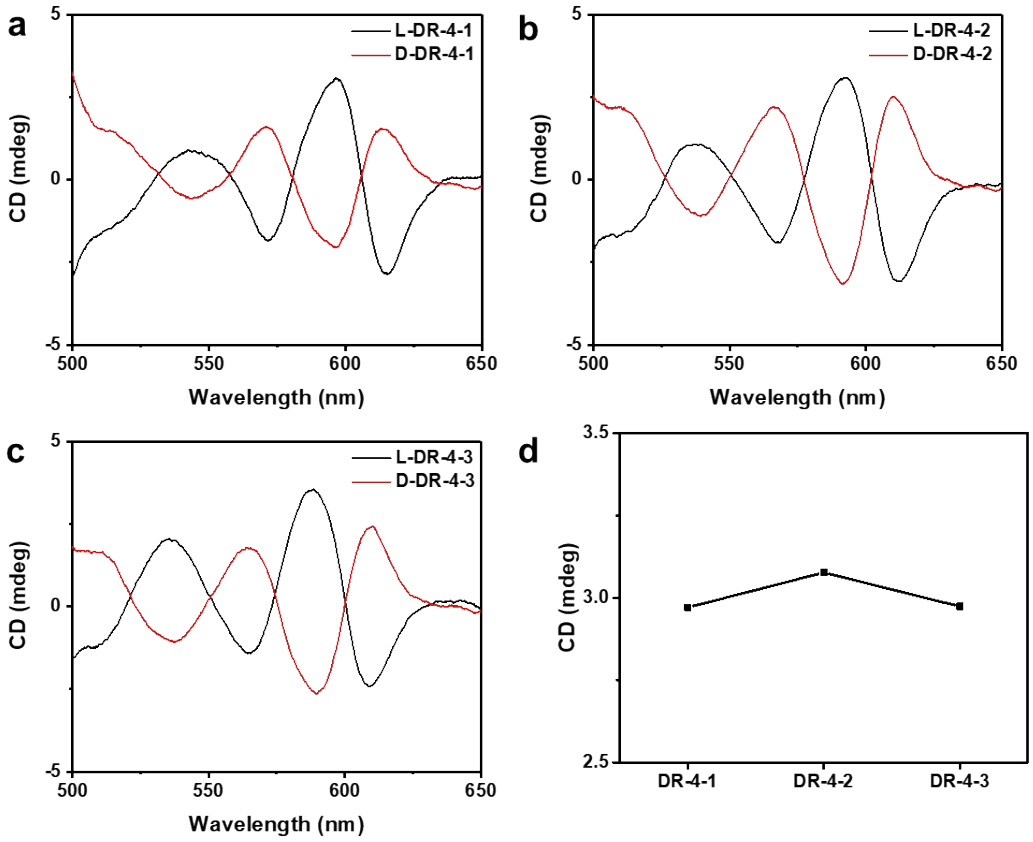

Figure S12. CD spectrum variations of DR-4-n (n =1-3) at the first exciton absorption peak during the etching process. a) CD spectrum of benzyl amine-modified DRs after the Cys exchange, b-c) CD spectra of DRs after one and two etching cycles and Cys exchange, d) CD signal evolution of L-Cys-DR-4-n (n =1-3) at the first exciton absorption peak during the etching process.

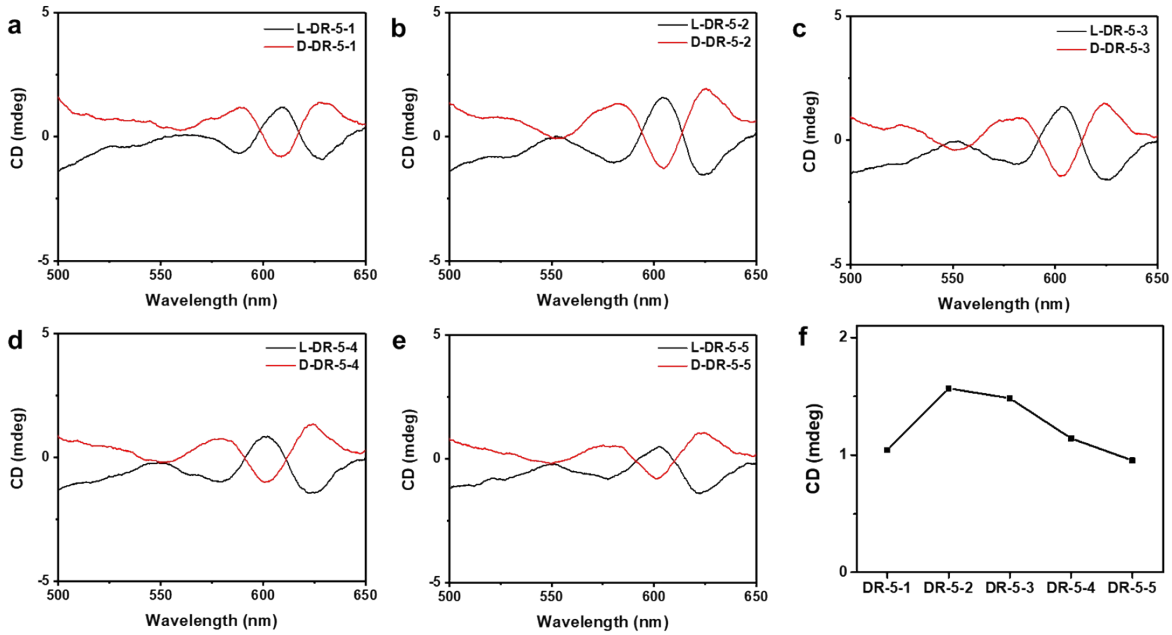

Figure S13. CD spectrum variations of DR-5-n (n = 1-5) at the first exciton absorption peak during the etching process. a) CD spectrum of benzyl amine-modified DRs after the Cys exchange, b-e) CD spectra of DRs after one cycle to four etching cycles and Cys exchange, f) CD signal variation of L-Cys-DR-5-n (n = 1-5) at the first exciton absorption peak during the etching process.

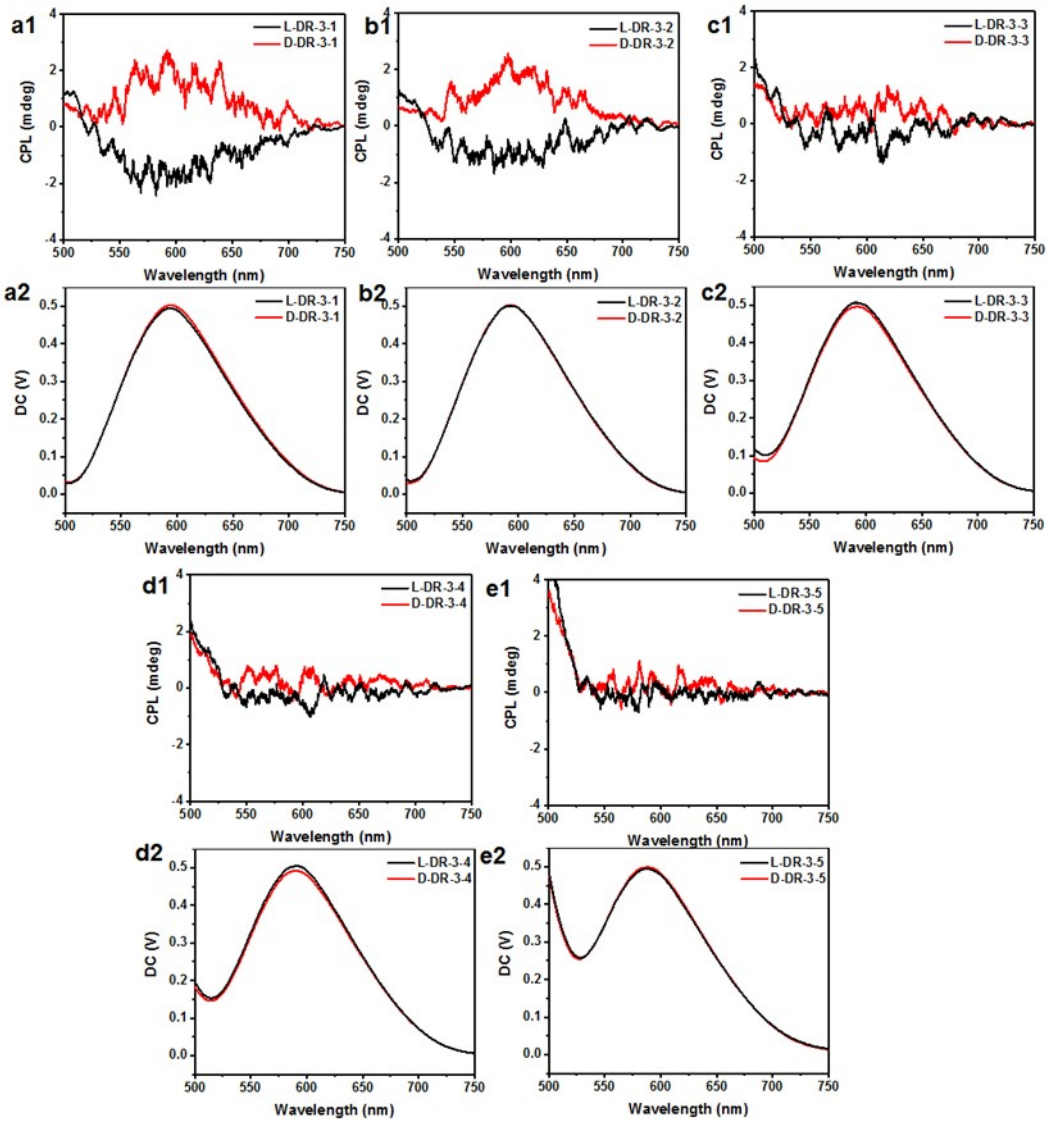

Figure S14. CPL variation of DR-3-n (n = 1-5) during the etching process. a1) CPL of benzyl amine-modified DRs after Cys exchange; b1-e1) CPL of DRs after one to four etching cycles and Cys exchange. a2-e2) Corresponding DC in volts, which stands for fluorescence intensity.

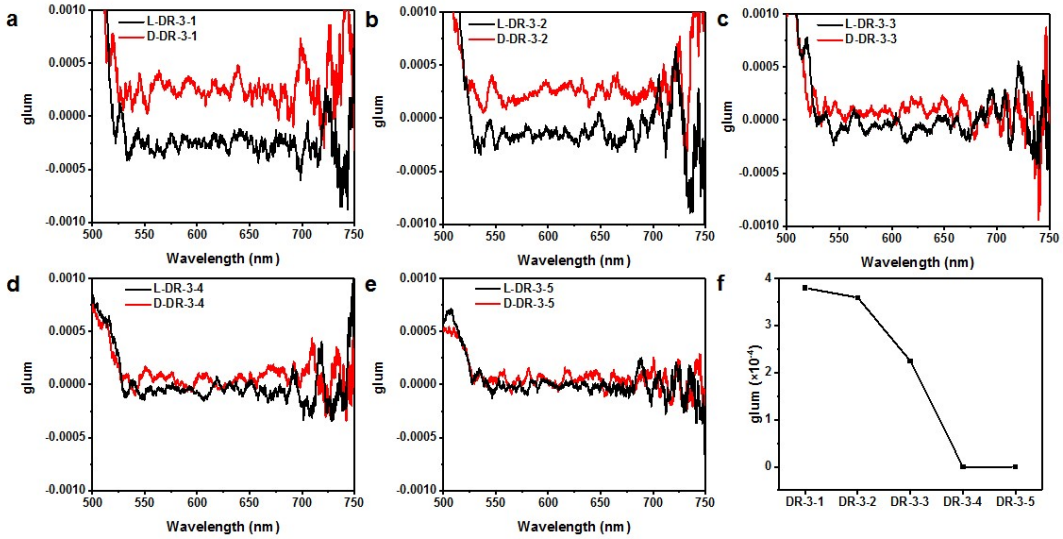

Figure S15. The corresponding g_{lum} variation of DR-3-n (n = 1-5), as shown in Figure S11. (a) The glum of benzyl amine-modified DRs after Cys exchange; (b)-(e) the g_{lum} of DRs after one to four etching cycles and Cys exchange; (f) the g_{lum} variation of L-Cys-DR-3 during the etching process.

1. W. W. Yu, L. Qu, W. Guo and X. Peng, Experimental Determination of the Extinction Coefficient of CdTe, CdSe, and CdS Nanocrystals, *Chem. Mater.*, 2003, **15**, 2854-2860.